Supporting information for "Parasite-driven cascades or hydra effects: susceptibility and foraging depression shape parasite-host-resource interactions"

Contents

Section 1: Additional model details

(a) Mortality-only model of predator-driven, density-mediated trophic cascades

When parasites only increase mortality (equation 1 with $\alpha = 0$; Fig. S1), the trophic cascade pattern that emerges follows that driven by predators. To make that point, consider a model of a logistically growing resource (R), a prey (S) that consumes the resource, and a predator (P) that consumes the prey. It provides a tractable comparison:

$$\frac{dR}{dt} = rR\left(1 - \frac{R}{K}\right) - f_0 SR \qquad \text{(S1a)}$$

$$\frac{dS}{dt} = cf_0SR - dS - f_PSP \qquad \text{(S1b)}$$

$$\frac{dP}{dt} = c_Pf_PSP - d_PP \qquad \text{(S1c)}$$

As in the model for parasites, resources grow logistically with intrinsic rate of increase r and carrying capacity K (equation S1a). Resources are consumed by prey (S, to mirror the model); these prey forage at per-capita rate f_0 (equation S1a). Consumed resources are converted into prey with efficiency c (equation S1b). Prey die at background per-capita rate d (equation S1b), and predators eat them at per-capita attack (capture) rate, f_P (equation S1b). Consumed prey are converted into predators with efficiency c_P (equation S1c). Predators die at background per-capita rate d_P. This minimal model assumes linear functional forms for clear analytical and dynamical interpretation – and for easier comparison to the disease analogue here. Other predator-prey-resource models consider further biological detail, such as Type II functional responses and metabolic types (Shurin & Seabloom 2005).

Due to their structural similarities, this model for predators yields predictions analogous to those of parasite-driven trophic cascades. Carrying capacity (K) has the same interpretation as a driver of resource productivity in both models (since it pertains to a logistically growing resource in both cases); susceptibility (u) acts similarly to attack rate of predators (f_P). Therefore, it is useful to determine the effects of carrying capacity (K) and attack rate of predators on resource and prey density without (R^*_{P-}, S^*_{P-}) and with (R^*_{P+}, R^*_{P+}, respectively) predators, and on the ratios of resources (R^*_{P+} / R^*_{P-}) and prey (S^*_{P+} / S_{P-}) with and without predators:

$$R^*_{P-} = \frac{d}{cf_0} \qquad \text{(S2a)}$$

$$R^*_{P+} = K\left(1 - \frac{f_o d_P}{c_P f_P r}\right) = \frac{d + f_P P^*}{cf_0} \qquad \text{(S2b)}$$

$$P^* = \frac{cf_0K\left(1-\frac{f_0 d_p}{c_P f_P r}\right)-d}{f_P} = \frac{cf_0}{f_P}(R^*_{P+} - R^*_{P-}) \qquad \text{(S2c)}$$

$$\frac{R^*_{P+}}{R^*_{P-}} = \frac{cf_0K}{d}\left(1-\frac{f_0 d_p}{c_p f_p r}\right) = \frac{d+f_P P^*}{d} \qquad \text{(S2d)}$$

$$S^*_{P-} = \frac{r}{f_0}\left(1-\frac{d}{cf_0K}\right) = \frac{r}{f_0 K}(K - R^*_{P-}) \qquad \text{(S2e)}$$

$$S^*_{P+} = \frac{d_P}{c_P f_P} = \frac{r}{f_0}\left(1-\frac{d+f_P P^*}{cf_0K}\right) = \frac{r}{f_0 K}(K - R^*_{P+}) \qquad \text{(S2f)}$$

$$\frac{S^*_{P+}}{S^*_{P-}} = \frac{cf_0^2 K d_p}{c_p f_p r(cf_0K - d)} = \frac{K - R^*_{P+}}{K - R^*_{P-}} \qquad \text{(S2g)}$$

Predators (P) increase prey mortality, thus they increase the minimal resource requirements (R^*) of their prey (S). Therefore, resource density with predators (R^*_{P+}) must be higher than without predators (R^*_{P-};,compare equation S2a and S2b). Carrying capacity (K) does not increase resources without predators because R^*_{P-} is the ratio of background mortality (d) to per-resource fecundity (cf_0; equation S2a). With predators, R^*_{P+} is linearly proportional to K. Biologically, R^*_{P+} increases with predators (P^*; equation S2c) because higher mortality increases minimum resource requirement of the prey (equation S2b). Thus, K amplifies release of resources by predators ($\mathrm{d}/\mathrm{d}K\,[R^*_{P+}/R^*_{P-}] > 0$; equation S2d). Additionally, attack rate of the predator (f_P) does not affect resources without predators (equation S2a) but increases it with them (equation S2b). Thus, f_P also amplifies resource release by predators ($\mathrm{d}/\mathrm{d}f_P\,(R^*_{P+}/R^*_{P-}) > 0$; equation S2d). Overall, resource release by predators with K and f_P in this model and a more complex one (Shurin & Seabloom 2005) mirror the (indirect) effects of parasites on resources of hosts.

Because they increase minimal resource requirements of their prey, predators suppress density of their prey. Prey density with predators (S^*_{P+}, proportional to $K - R^*_{P+}$) must be lower than that without predators (S^*_{P-}, proportional to $K - R^*_{P-}$; compare eqs. S2e and S2f). Carrying

capacity (K) increases prey without predators because prey enjoy top-down control of resources (equation S2e). With predators, prey become fixed at the minimum prey requirement of predators and therefore cannot increase with K (equation S2f). Thus, K amplifies how much predators harm prey density ($d/dK\ [S^*_{P+}/S^*_{P-}] < 0$ always; equation S2g). Increasing attack rate of predators (f_P) decreases prey density with predation (since f_p increases R^*_{P+}; equation S2f). Thus f_P amplifies how much predators suppress prey ($d/df_P\ [S^*_{P+}/S^*_{P-}] < 0$; equation S2g). Consequently, the effects of predators on prey density via attack rate f_P mirror those of parasites on host density via susceptibility u in the mortality-only model case. Such analogous predictions only hold for carrying capacity when considering resource release. The victim suppression response instead differs between predators and prey (see below).

(b) Numerical search of parasite model and comparison to predator-driven cascades – Fig. S1, Table S1

To study the mortality-only case of the disease model, we needed to use numerical approaches. Intuitively, higher susceptibility (u) and carrying capacity (K) should lead to higher prevalence of infection (p). Also, it seems that higher K should increase host density with disease (H^*_{Z+}; as long as K doesn't increase p^* very fast: see equation S3e). Because the expressions involved are very large (hence opaque), we evaluated equilibrium quantities along broad parameter ranges, from 10^{-2} to 10^2 x default parameter values (see Table 1). We divided these ranges into 10^4 evenly spaced values, then used a Latin Hypercube search (McKay, Beckman & Conover 2000) to find equilibrium densities at each parameter combination. At each parameter set, we increased or decreased K or u 10% to determine its effect on equilibria, without ($\alpha = 0$) and with foraging depression ($\alpha > 0$). Without foraging depression, higher K or u always

increased prevalence, and higher K always increased host density with disease. With foraging depression, prevalence can decrease with K (but only increased in our focal parameter range: see Fig. S1a and Table 1). Additionally in eight of 10^4 parameter sets, u can decrease prevalence (e.g., c = 1.318302 x 10^1, f_0 = 9.865147 x 10^{-1}, α = 3.061821 x 10^{-04}, u = 3.486 x 10^{-06}, d = 3.702714 x 10^{-1}, v = 3.087158, s = 3.247983 x 10^6, r = 1.916043 x 10^1, K = 9.410805 x 10^3, m = 1.191349 x 10^2). Additionally, in two of 10^4 parameter sets, K can decrease host density with disease (e.g., c = 8.051979, f_0 = 1.338437, α = 2.285137 x 10^{-4}, u = 4.82811 x 10^{-4}, d = 2.285037 x 10^{-1}, v = 2.215772 x 10^{-1}, s = 3.624676 x 10^6, r = 1.253682 x 10^{-1}, K = 8.735303 x 10^3, m = 1.290146 x 10^2). So, in the majority of cases and always within the biologically relevant range of parameter values, the intuitive effects of K and u on prevalence and host density hold.

With their relationships to prevalence established, we then evaluated the effects of u, K, and parasites on resource and host density with or without disease. With those densities, we calculated ratios (and related $\log_{10}$ of density ratios), common metrics of cascade strength (Shurin *et al.* 2002; Shurin & Seabloom 2005). With these metrics, cascades become stronger with smaller (log) ratio of hosts and higher (log) ratio of resources, i.e., with stronger host suppression and resource release, respectively. For the simple case where $\alpha = 0$ (see equation 2 more generally), these quantities are:

$$R^*_{Z-} = \frac{d}{cf_0} \qquad \text{(S3a)}$$

$$R^*_{Z+} = \frac{d + vp^*}{cf_0} \qquad \text{(S3b)}$$

$$\frac{R^*_{Z+}}{R^*_{Z-}} = \frac{d + vp^*}{d} \qquad \text{(S3c)}$$

$$H^*_{Z-} = \frac{r}{f_0}\left(1 - \frac{d}{cf_0K}\right) = \frac{r}{f_0}\left(1 - \frac{R^*_{Z-}}{K}\right) \qquad \text{(S3d)}$$

$$H^*_{Z+} = \frac{r}{f_0}\left(1 - \frac{d + vp^*}{cf_0K}\right) = \frac{r}{f_0}\left(1 - \frac{R^*_{Z+}}{K}\right) \qquad \text{(S3e)}$$

$$\frac{H^*_{Z+}}{H^*_{Z-}} = \frac{cf_0K - d - vp^*}{cf_0K - d} \qquad \text{(S3f)}$$

Because parasites increase host mortality, they increase the minimum resource density required by hosts (a ratio of losses to per resource gains of hosts) from R^*_{Z-} (equation S3a) to R^*_{Z+} (equation S3b). As carrying capacity (K) increases, infection becomes more prevalent (Fig. S1a), parasite propagules more abundant (Fig. S1b), and a greater difference between resources with parasites and without (equation S3a; Fig. S1c). Susceptibility (u) does not affect resource density without disease (dashed lines are flat; Fig. S1c) but increases resource density with disease by elevating prevalence (solid curves increase with u; Fig. S1c). Hence, the resource density ratio increases with both carrying capacity and susceptibility [equation S3c; d/dK (R^*_{Z+}/R^*_{Z-}) > 0, red curve sits above the blue one; d/du $R^*_{Z+}/R^*_{Z-} > 0$, curves increasing with u-axis: Fig. S1d]. Stated simply, both higher u and K lead to larger resource release.

In this mortality-only model case, parasites can only suppress host density. Mathematically, mortality increases the minimum resource requirement, $R^*_{Z+} > R^*_{Z-}$, so host density declines, $H^*_{Z+} < H^*_{Z-}$ (see eqs. S3d, e; solid line below dashed one in Fig. S1e). Carrying capacity (K) increases host density without or with parasites (both $dH^*_{Z-}/dK > 0$ [analytically] and $dH^*_{Z+}/dK > 0$ [in numerical searches]; dashed red curve lies above dashed blue [Fig. S1e]). However, K may increase or decrease the host ratio (the increase example where K weakens host suppression, d/dK [H^*_{Z+}/H^*_{Z-}] > 0, is shown with red curve above blue in Fig. S1f). Susceptibility (u) does not affect host density without disease (equation S3d; flat H^*_{Z-} curves, Fig. S1e), but decreases it with disease through increasing prevalence (p^*; equation S3e; decreasing H^*_{Z+} curves, Fig. S1e). So, higher susceptibility increases host suppression (equation S3f decreases;

curves decreasing in Fig. S1f). Summarizing, in the mortality-only model case, parasites suppress host density more strongly when hosts have higher susceptibility but not necessarily when carrying capacity is higher. Allowing foraging depression in the parasite model ($\alpha > 0$) does not qualitatively change these patterns for hosts and resources.

The mortality-only model case shows that parasite-driven, density-mediated trophic cascades should function mostly like predator-driven, density-mediated ones (Section 1a; equation S1, S2). Parasites that only increase mortality can only suppress host density and release resources. The resource release (higher resource ratio, R^*_{Z+}/R^*_{Z-}) and host suppression (lower host ratio, H^*_{Z+}/H^*_{Z-}) both become stronger with higher susceptibility, u (analogous to predator attack rate). Resource ratio also increases with carrying capacity, K, in both disease and predator-driven cascades. However, host ratio increases or decreases with K; its analogue only decreases with K in predator-driven cascades. This difference arises because infected hosts accumulate with K whereas predators fix prey density at their minimal requirement, a value unchanging with K. Predators fix density of their prey at their minimal prey requirement: $S^*_{P+} = d_P/[c_P f_P]$; equation S2f). In contrast, host density (S+I) still increases with K during epidemics due to accumulation of infected hosts (I), even though the parasite itself has a minimal requirement for susceptible hosts itself ($S^*_{Z+} = m / [u f_0 \sigma]$, a ratio of losses to gains like that of the predator). Because this accumulation of I allows host density (S+I) to increase with K, host ratio (equation S3f) can increase or decrease with K. The case with predators is simpler: captured prey are immediately removed by predators, so prey ratio (equation S2g) can only decrease with K. Otherwise, the mortality-only case (equation 1 with $\alpha = 0$) and predator model (equation S1) produce analogous predictions for strength of trophic cascades. Thus, when parasites only kill, density-mediated trophic cascades largely resemble those with predators, yielding predictable

effects of susceptibility, nutrient supply, and disease in the experiment (Table S1).

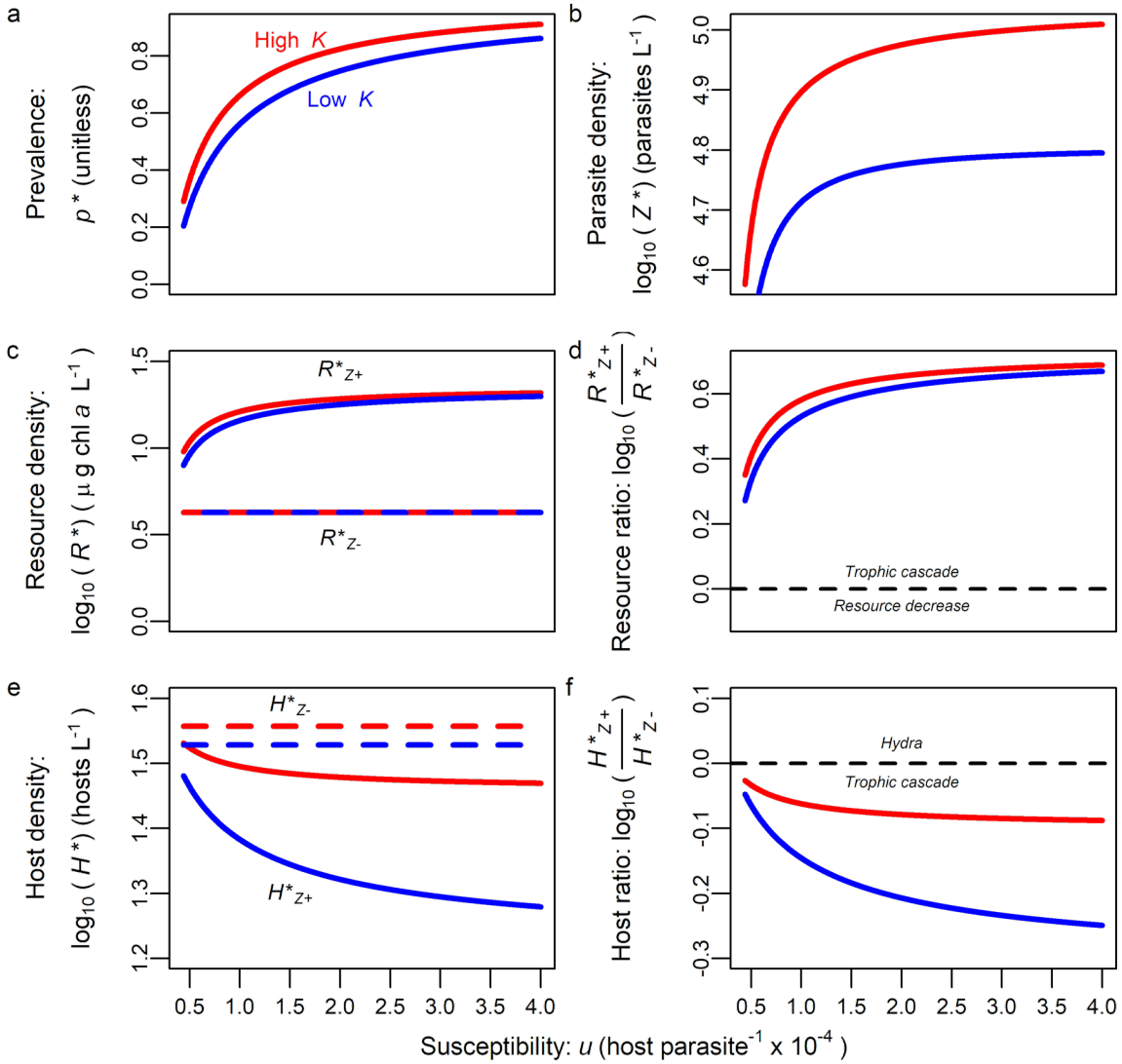

Figure S1. *Predicted effects of susceptibility on cascade strength at equilibrium in mortality-only case (eqs. 1, S3).* (a) Higher susceptibility (u) and carrying capacity (K) both lead to higher prevalence (p^*) of infection (b) and increased density of parasite propagules (Z^*). (c) Without disease (dashed lines), resource density is fixed at the minimum requirement of the host (R^*_{Z-}) and unaffected by susceptibility, u, or carrying capacity, K. With disease (solid curves), resources (R^*_{Z+}) increase above R^*_{Z-} with u and K. (d) Resource ratio: densities of resources with

and without disease. Values above zero on a $\log_{10}$ scale indicate trophic cascade; below zero, resources decrease (which cannot occur in this model). Resource ratio increases with both u and K (both curves increasing and red curve above blue). (e) Without disease, susceptibility does not affect host density (H^*_{Z-}). With disease (solid), total host density (H^*_{Z+}) decreases with susceptibility. Higher K leads to higher host densities (red curves above corresponding blue). (f) Host ratio: densities of hosts with and without disease (H^*_{Z+} / H^*_{Z-}). Values below zero on a log scale indicate trophic cascade; above zero indicate a hydra effect. Host ratio decreases with u (both curves decreasing) but not necessarily with K (e.g., blue curve below red in this example). Together, (a), (d), and (f) show that trophic cascade strength increases with u as disease spreads more easily. K = 20 (low) or 94.3 (high) μg chl *a*/L; other parameter values listed in Table 1.

(c) Outcomes other than one stable equilibrium in the main model (equation 1)

Oscillations: The model analyzed in the main text can produce oscillations instead of a stable interior equilibrium whether or not foraging depression occurs. These oscillations can arise when the carrying capacity of the resource (K) is very high (e.g., all parameters default except K = 377, a value far beyond the maximum here [K = 100]). High K weakens negative density dependence of the resource, which is usually a stabilizing factor. However, other feedback loops may also be involved in the genesis of oscillations (and a detailed decomposition of the complex stability criterion for them exceeds the point of this present paper). Foraging depression tends to reduce the possibility for oscillations, but they may still arise (e.g., high K = 472 and weak $\alpha = 3.455 \times 10^{-7}$, all others as default, see Table 1).

Multiple stable equilibria: All plots presented in the main text use parameter ranges that give only one stable equilibrium. In contrast, foraging depression ($\alpha > 0$) does allow two

simultaneously stable equilibria. Positive feedbacks between parasites and host density can create alternative stable states. For some parameter values (e.g. $c = 22.5$, $d = 0.0176$, $f_0 = 0.0161$, $K = 265$, $m = 9.59$, $u = 1.66 \times 10^{-4}$, $v = 0.19$, $w = 8.39$, $\alpha = 7.50 \times 10^{-8}$, $\sigma = 7.75 \times 10^{4}$), two endemic equilibria can be stable. A low disease equilibrium has lower parasite propagule density, higher foraging rate, lower resource density, lower primary productivity, and lower host density. If instead parasite propagules are denser, host foraging rate is strongly depressed (because $\alpha > 0$), resources are denser and more productive and thus support a larger host population with lower prevalence. These alternative stable states arise because of positive feedbacks between parasite propagule density and host density. If hosts have low density, parasite propagules will be sparse, and hosts will have a high foraging rate. This high foraging rate keeps host density low by overgrazing resources. If hosts become denser, however, parasite propagule density increases, depressing host foraging rate and increasing host density. Further theoretical exploration could more clearly demonstrate the feedbacks, biological feasibility, and dynamical implications of this bistability.

(d) Hydra effects and cascades with susceptibility (u) – Fig. S2 showing slices of α in Fig. 3c, d

Increasing susceptibility (u) to infection can promote disease, counterintuitively increasing host density if it amplifies a hydra effect. Generally, increasing u amplifies the negative impact of parasites on host populations (host suppression). But, if there is already a hydra effect, increasing u can amplify that hydra effect. Increasing susceptibility, u, increases density of parasite propagules, Z^*, particularly with higher levels of foraging depression, α (Fig. S2a). Therefore, foraging rate of hosts drops with u (more Z) and α (stronger sensitivity to Z; Fig. S2b). Since epidemics become larger with u, resource density (i.e., the host's minimal

213 requirement) increases with u. It also increases further with sensitivity of foraging depression
214 (higher α: Fig. S2c). If the minimal resource requirement of the host without disease (R^*_{Z-}) lies
215 below $K/2$ (density at peak resource productivity), the increase in resource density with disease
216 (to R^*_{Z+}) can increase productivity of the resource (where again, $PP = r\,R^*\,(1 - R^*/K)$; Fig. S2d).
217 Parasites that depress host foraging, then, have a stronger effect on PP than food consumption
218 (FC). Notice, however, that the effects of foraging depression on per host food consumption,
219 $f(Z^*)\,R^*_{Z+}$, almost completely cancels; food consumption increases more with u than with α (Fig.
220 S2e).

221 Host density (H^*; Fig. S2f) is the ratio of PP to food consumption. Two patterns emerge.
222 First, hydra effects are more likely at higher α because it increases PP with small effect on
223 consumption. Conversely, when α is small, the PP boost from epidemics is smaller - too small to
224 cause a hydra effect given the increase in consumption. So, instead, a cascade arises. At
225 intermediate α, we find a shift with increasing u from hydra effect to cascade (as consumption
226 increases faster with u than PP). If hosts do not depress their foraging rate ($\alpha = 0$, or if $R^*_{Z-} >$
227 $K/2$), then increasing susceptibility always decreases host density. Second, when a hydra effect is
228 possible, it may be strongest (i.e., peak in host ratio) at intermediate u. At this level of u, parasite
229 propagules (Z) become dense enough to reduce foraging rate while not adding too much
230 mortality for hosts.

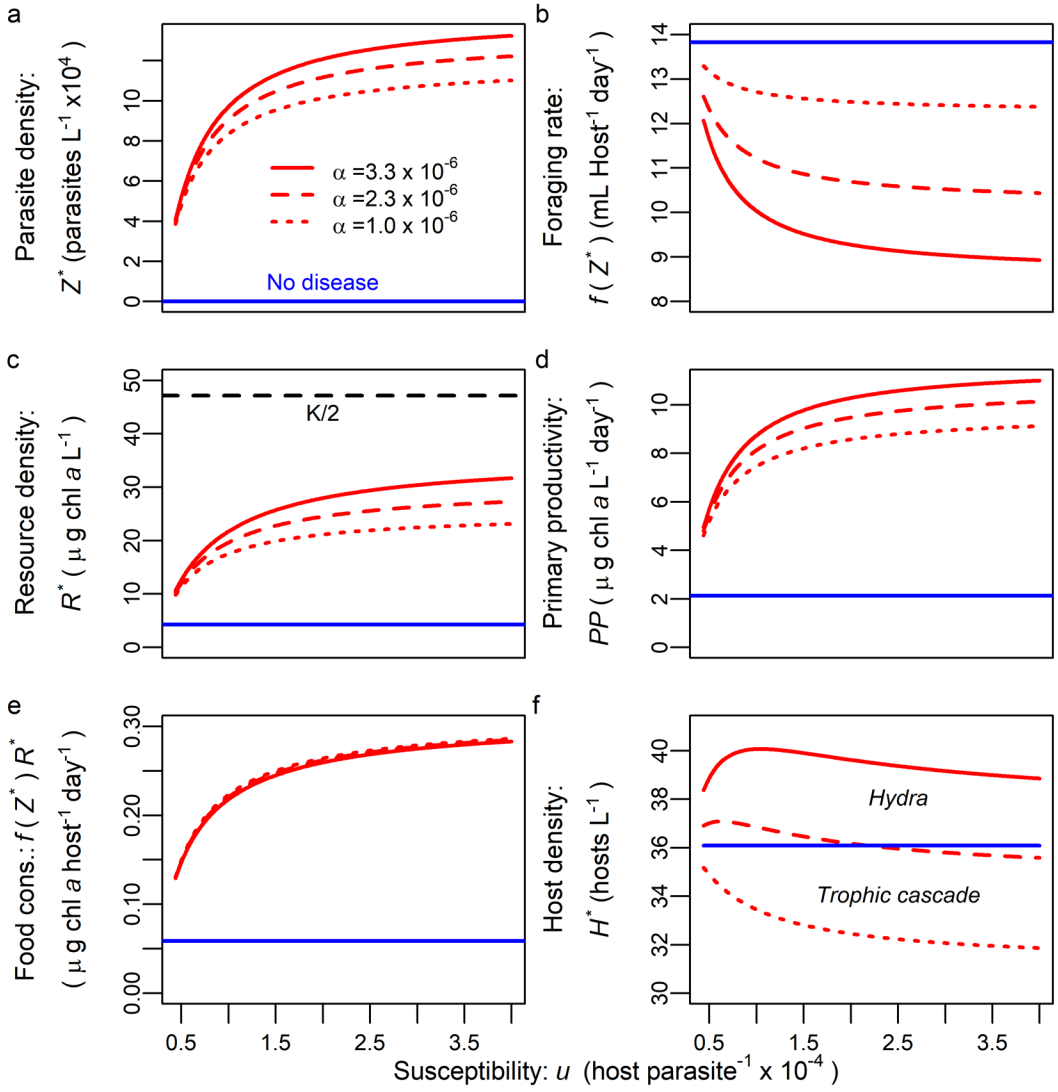

231

232 **Figure S2.** *Hydra effects and cascades with susceptibility (u) and different foraging depression*
233 *(α).* Values of foraging depression (contours) here correspond to horizontal slices of Figs. 3c, d.
234 (a) Higher susceptibility (u) leads to higher parasite propagule density with disease (red) but has
235 no effect without it (blue). Higher foraging depression (α) can increase parasite propagule
236 density (Z^*) due to associations with host density (red contours). (b) Higher Z with increasing
237 susceptibility depresses foraging rate, $f(R^*)$, particularly when α is larger. (c) Resource density,
238 R^*, increases with susceptibility as more hosts are infected (higher p^* with u) and each host

239 forages less. Increased resources (R^*_{Z+}) can be closer to $K/2$ (where production is maximized;
240 dashed black line). (d) Because R^*_{Z+} becomes closer to $K/2$, primary productivity, PP, increases
241 with u and α. (e) Food consumption, $f(Z^*)R^*$, rises with higher u to compensate for more
242 mortality but increases less for higher α. (f) If foraging depression is strong enough (solid and
243 dashed red), higher susceptibility can lead to increased host density ($H^*_{Z+} > H^*_{Z-}$, hence a hydra).
244 Even so, host density reaches a maximum at intermediate susceptibility. Higher susceptibility
245 decreases foraging rate slightly (via increased Z^*; panel b) but increases mortality. Thus,
246 increased susceptibility can drive a transition from hydra effect to trophic cascade (dashed red).
247 [$\alpha = 3.3 \times 10^{-6}$ (solid), 2.3×10^{-6} (dashed), 1.0×10^{-6} (dotted); see Table 1 for other parameter
248 values].
249

250 ***(e) Higher virulence (v) and cascades vs. hydra effects – Fig. S3***

251 The outcome of trophic cascade or hydra effect depends on a tension between mortality
252 and foraging depression. Higher virulence mortality (v) of parasites increases direct harm to host
253 fitness, more strongly increasing resource density (i.e., the minimal resource requirement of
254 hosts, R^*_{Z+} [equation 2b]; Fig. S3a). Higher foraging depression also increases resource density
255 (Fig. S3a; hence, resource ratio increases up and to the right). Higher virulence tends to depress
256 host density (equation 2d; Fig. S3b; host ratio mostly declines to the right). Increasing foraging
257 depression increases host density and can drive a hydra effect (Fig. S3b; trophic cascade below
258 black curve and hydra effect above). With higher virulence, stronger foraging depression is
259 required to still give a hydra effect (black line increasing in Fig. S3b). Once in v-α space
260 producing a hydra effect, a different pattern can arise. At high α, increasing virulence can
261 sometimes amplify an existing hydra effect (host ratio increasing with v for $\alpha = 3.5 \times 10^{-6}$). Here,

higher virulence increases conversion of infected hosts into parasites, which depress foraging rate. (This result assumes that propagule yield per infected host, σ, would not change with v, an unlikely assumption biologically). With high enough α but not too high (not shown), this extra foraging depression can increase host density further. Generally, however, higher mortality virulence decreases host density because v increases food consumption more than primary productivity. Furthermore, in a numerical search of equilibrium densities, higher v never increases host density in the mortality-only model case ($v > 0$ but $\alpha = 0$). In terms of our pattern from hydra effects to trophic cascades, higher virulence does not seriously undermine this pattern. Populations with low susceptibility and strong foraging depression keep prevalence low. Hence, they suffer little from increased virulence, maintaining hydra effects. In contrast, populations with high susceptibility and low foraging depression suffer high prevalence. The large, population-level effects of increased virulence magnify host depression and resource release.

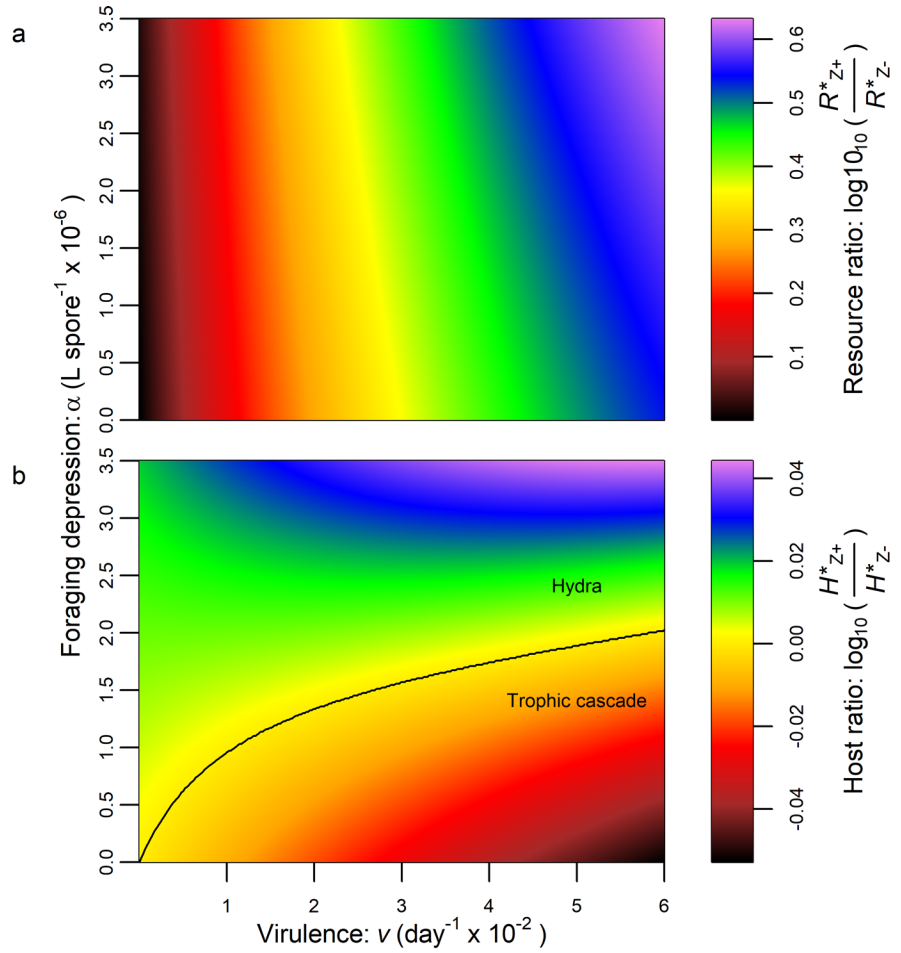

Figure S3. *Higher virulence (added mortality from infection) makes it harder for parasites to drive a hydra effect.* Mortality virulence ($v > 0$) kills more hosts (all else equal), leading to a trophic cascade. Foraging depression can still increase productivity enough to overwhelm this mortality effect and drive a hydra effect. (a) Both virulence and foraging depression increase resource release ($\log_{10}$ of resource ratio, R^*_{Z+} / R^*_{Z-}). (b) Higher virulence, v, generally suppresses host density (decreases $\log_{10}$ of host ratio H^*_{Z+} / H^*_{Z-}) while foraging depression increases host ratio. Hydra effects (above black line), therefore, are more likely for less virulent parasites that depress foraging [black line, where $\log_{10}(H^*_{Z+} / H^*_{-}) = 0$, increases with v]. See Table 1 for parameter values.

(f) Time series of model simulations and mesocosm data

We also ran simulations with two genotypes to match two-genotype populations. We do this simply with a host population composed of a 50:50 ratio of individuals from the two clones (see Discussion for future exploration of evolution of these traits). Thus, average foraging rate for a population at this 50:50 ratio is given by $f_{av} = f_0[\exp(-\alpha_1 Z) + \exp(-\alpha_2 Z)]/2$ while average transmission rate is given by $\beta_{av} = f_0[u_1\exp(-\alpha_1 Z) + u_2\exp(-\alpha_2 Z)]/2$. With populations of two clones, simulations still adhere closely to the equilibrium, model patterns (see Figs. S4, S6).

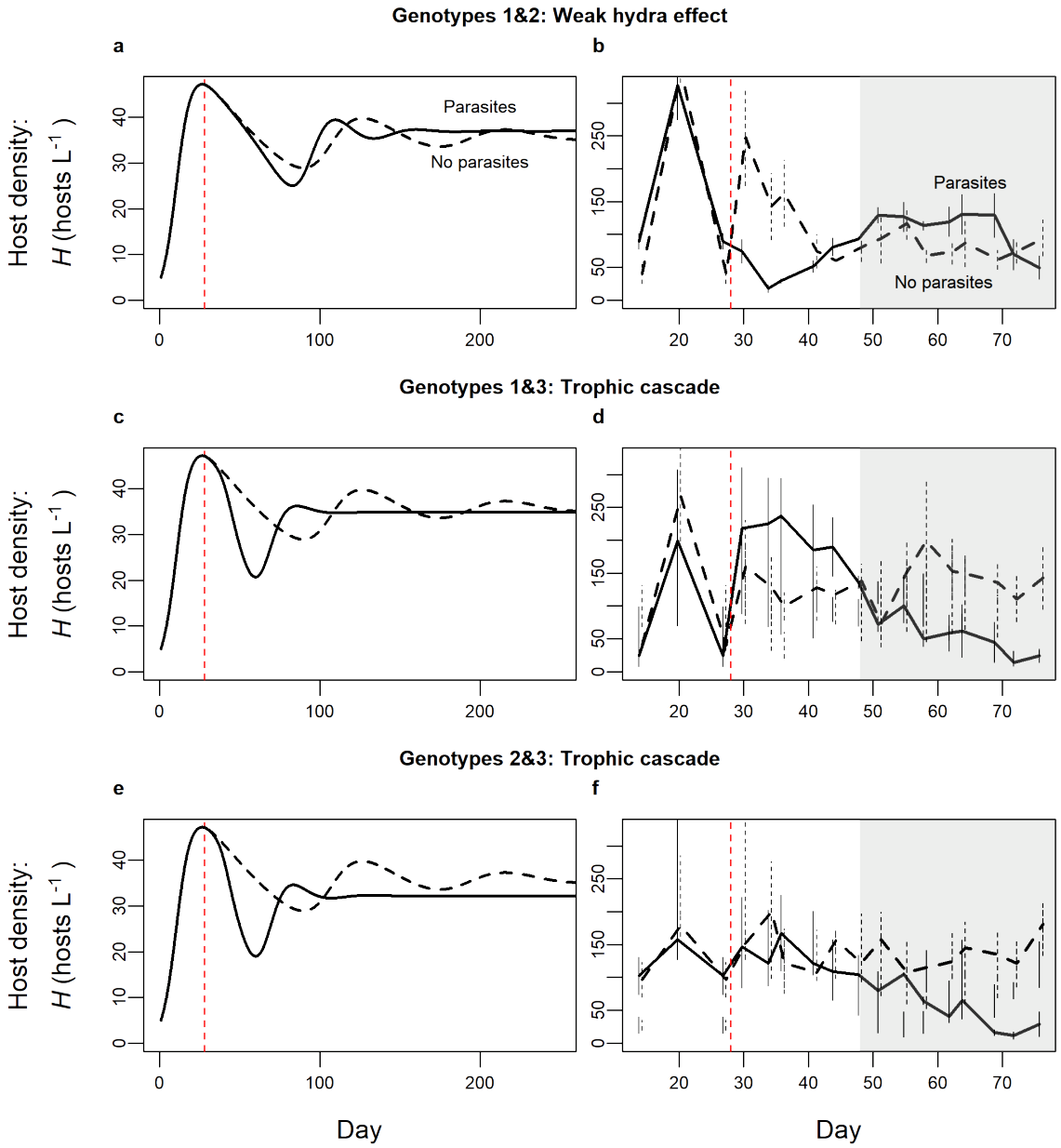

Figure S4. *Simulated and experimental time series at high nutrients (*K = *94.3 in simulations or 50 µg L^{-1} P in mesocosms) produce a spectrum ranging from hydra effects to trophic cascades for two-genotype populations.* In both simulations and the experiment, hosts and parasites are added on days 1 and 28 (red tick mark), respectively. (a) With genotypes 1&2 present, the hydra effect emerges given sufficient time as host density with parasites (solid) becomes higher than

without (dashed). (b) Mesocosms containing genotypes 1 & 2 experienced a hydra effect [mean density across replicates with parasites (solid) or without (dashed), plotted at each time point; bars are standard error at each time point]. (c-f) With genotypes 1&3 or 2&3, a trophic cascade occurs in simulations and the mesocosm. (Parameters follow Table 1). For analyses, average mesocosm density was taken from day 48 to 76 (gray region, see Appendix: section 2c). Experimental time series shifted slightly horizontally for clarity. Compare simulations to Fig. 3's equilibrium outcomes and mesocosm time series to Fig. 5's mesocosm averages.

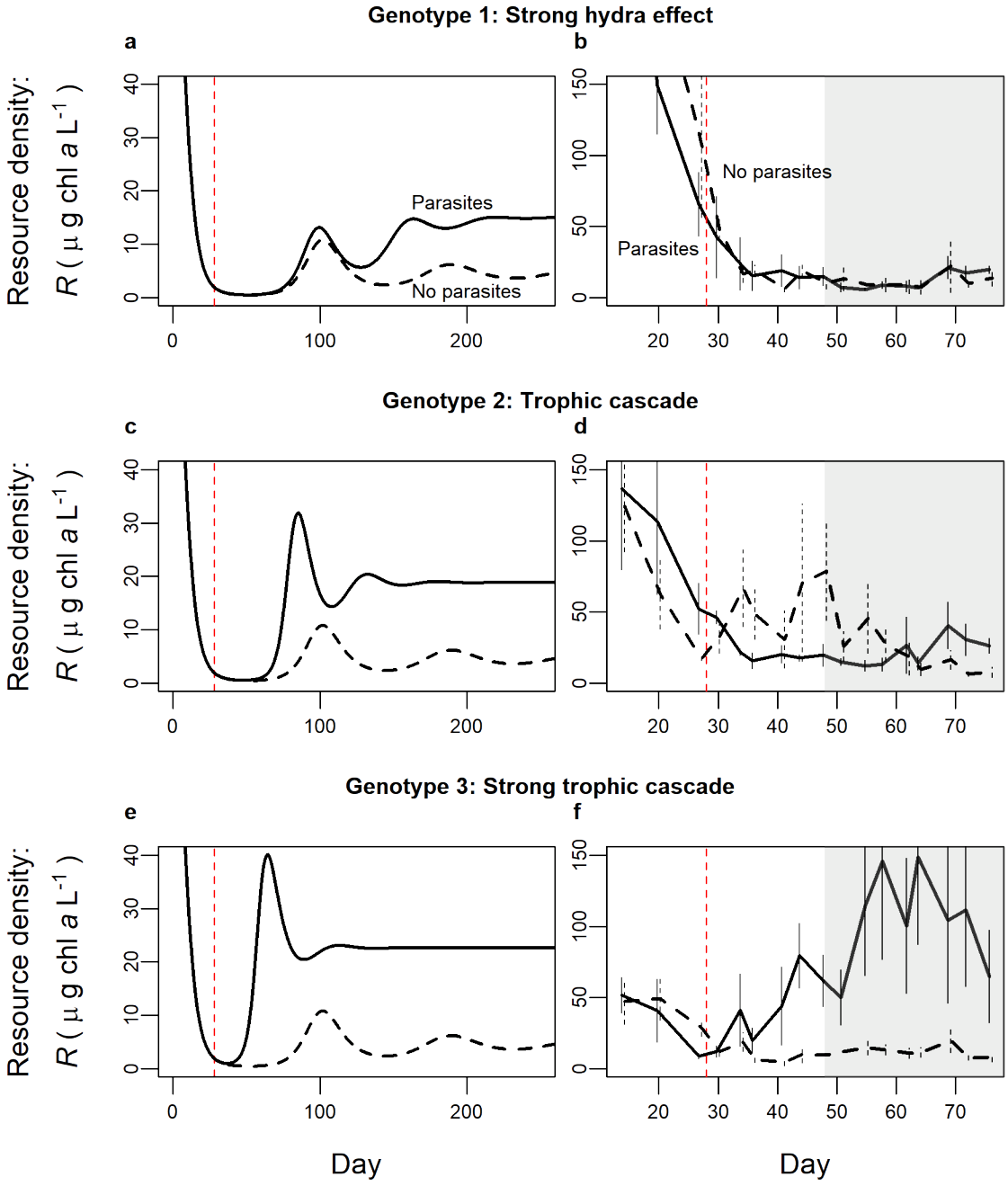

312

313 **Figure S5.** *Resource density in simulation and mesocosm time series for single-genotype*

314 *treatments at high nutrients (*K = *94.3 in simulations or 50 µg L-1 P in mesocosms).* Resource

315 release (one measure of cascade strength) compares resources with parasites (solid) to without

316 (dashed). Treatments with stronger foraging depression and lower susceptibility experience
317 smaller resource release in simulations (a) and mesocosms (b). Treatments with weaker
318 depression and higher susceptibility (c-f) experience larger resource release, largely due to
319 killing of hosts. For analyses, average mesocosm density was taken from day 48 to 76 (gray
320 region, see Appendix: section 2c). Experimental time series shifted slightly horizontally for
321 clarity. Compare simulations to Fig. 3's equilibrium outcomes and mesocosm time series to Fig.
322 5's mesocosm averages.

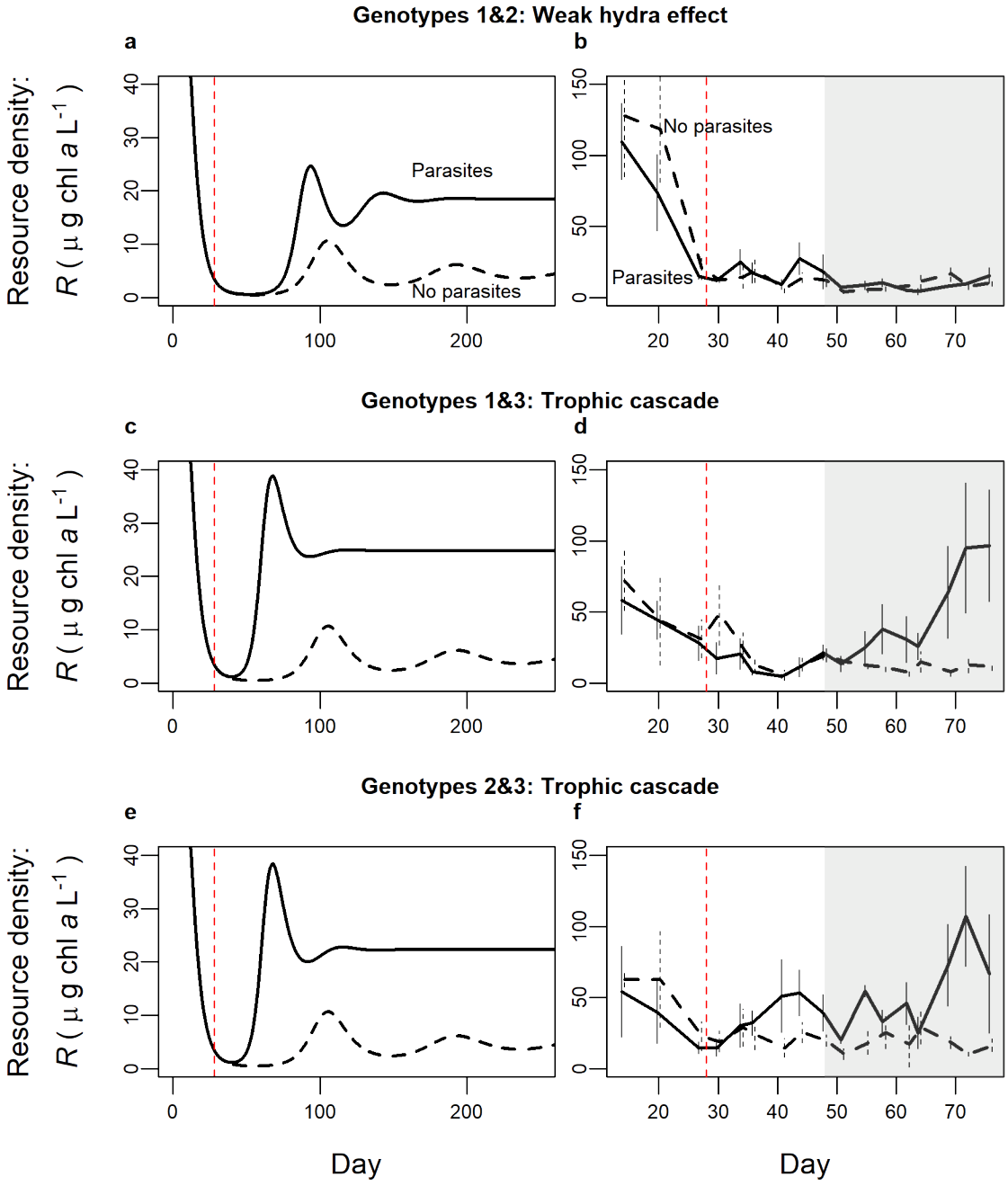

323

324 **Figure S6.** *Resource density in simulation and mesocosm time series for two-genotype*

325 *treatments at high nutrients (*K = *94.3 or 50 µg L-1 P).* Resource release is measured by

326 comparing resource density with parasites (solid) to without (dashed). For analyses, average

mesocosm density was taken from day 48 to 76 (gray region, see Appendix: section 2c). Experimental time series shifted slightly horizontally for clarity.

(g) Virulence on fecundity (θ) and cascades vs. hydra effects

Virulence on fecundity should accentuate trophic cascades. Many parasites reduce host fecundity (for several examples, see Ebert, Lipsitch & Mangin 2000), ranging from partial to full castration (no fecundity from infected hosts). The model can be easily altered to incorporate the possibility of fecundity reduction:

$$\frac{dR}{dt} = rR\left(1 - \frac{R}{K}\right) - f(Z)(S + I)R \qquad \text{(S4a)}$$

$$\frac{dS}{dt} = cf(Z)(S + \theta I)R - dS - uf(Z)SZ \qquad \text{(S4b)}$$

$$\frac{dI}{dt} = uf(Z)SZ - (d + v)I \qquad \text{(S4}c\text{)}$$

$$\frac{dZ}{dt} = \sigma(d + v)I - mZ \qquad \text{(S4d)}$$

The update introduces θ, relative fecundity of infected hosts. If $\theta = 1$, infected hosts have full fecundity (i.e., the assumption made before). If $\theta = 0$, parasites castrate fully: infected hosts consume resources [at rate $f(Z)$] but produce no offspring (hence, this model is not quite like the predator-prey analogue; equation S1). Fecundity reduction (θ) then alters equilibrium densities or resources, R^*_{Z+}, and hosts, H^*_{Z+} during epidemics (from eqs. 2b, d to S5):

$$R^*_{Z+} = \frac{d + vp^*}{cf(Z^*)(1 - p^* + \theta p^*)} = \frac{d + vp^*}{cf(Z^*)(1 - p^*) + \theta cf(Z^*)p^*} \qquad \text{(S5a)}$$

$$H^*_{Z+} = \frac{r}{f(Z^*)}\left(1 - \frac{R^*_{Z+}}{K}\right) \qquad \text{(S5b)}$$

where minimal resource requirement of hosts during epidemics, R^*_{Z+}, is the ratio of mortality (d

347 + vp) to per resource fecundity (equation S5a). However, notice that per resource fecundity now
348 differs for susceptible hosts, $cf(Z)$, and infected hosts, $cf(Z)\theta$, (weighted by frequencies of
349 susceptible [1-p^*] and infected [p^*] hosts, respectively). Host density, H^*_{Z+} (equation S5b)
350 remains similar before (compare to equation 2d), but with an updated value of R^*_{Z+} (equation
351 S5a; compare denominator here to denominator in equation 2b). We do not fully analyze this
352 model but provide intuitive predictions to be tested by future studies.
353 Fecundity reduction seems likely to reduce the possibility of a hydra effect compared to
354 the virulence on mortality. Fecundity reduction (represented by $\theta < 1$) reduces host fitness
355 overall, likely despite a small compensatory decrease in infection prevalence ($dp^*/d\theta < 0$).
356 Reduced host fitness increases the resources required for the host population to survive during
357 epidemics (increases R^*_{Z+}, compared to equation 2b). Increased R^*_{Z+}, all else equal, must increase
358 food consumption more than it increases primary productivity (because food consumption
359 increases linearly with R^* while PP increases less than linearly). This same reasoning explains
360 why mortality alone ($v > 0$, $\alpha = 0$, $\theta = 1$) must suppress host density. Thus, stronger castration
361 (decreasing θ) should further suppress host density (as found theoretically and empirically by
362 Ebert, Lipsitch & Mangin 2000 but without a dynamic resource).
363 Despite these insights, it seems unlikely that virulence on fecundity would undermine the
364 gradient from hydra effects to trophic cascades across genotypes. For instance, the combination
365 of low susceptibility with strong foraging depression still leaves low prevalence of infection.
366 Hence, virulence on fecundity should not have a great impact on such populations, leaving hydra
367 effects largely intact. Weak foraging depression and high susceptibility populations suffer high
368 prevalence so virulence on fecundity should amplify resource release and host suppression,
369 strengthening cascades. Virulence on fecundity may decrease prevalence, making these patterns

somewhat more complex. However, such feedback on prevalence would have to become quite strong to completely undermine the pattern that we saw across genotypes. Detailed modeling of these feedbacks remains beyond the scope of this paper.

(h) Foraging depression can produce hydra effects in a model with direct transmission

A model of direct transmission shows a parasite-driven hydra effect is not restricted to environmentally transmitted parasites. Here foraging depression functions in a similar manner, responding to the infectious stage (here I instead of Z, so α has different units): $f(I) = f_0 e^{-\alpha I}$. This modification yields a three-dimensional model:

$$\frac{dR}{dt} = rR\left(1 - \frac{R}{K}\right) - f(I)(S + I)R \qquad \text{(S6a)}$$

$$\frac{dS}{dt} = cf(I)(S + I)R - dS - uf(I)SI \qquad \text{(S6b)}$$

$$\frac{dI}{dt} = uf(I)SI - (d + v)I \qquad \text{(S6c)}$$

Because this model is not our focus and our system does not provide biologically reasonable parameter values, we conduct a brief, mostly numerical analysis. Similar to the mortality-only model, the equilibrium host density (H^*) cannot become higher during epidemics without foraging depression ($H^*_{Z+}/H^*_{Z-} < 1$ for $\alpha = 0$). Numerical analysis readily shows a hydra-like effect can arise when $\alpha > 0$ (e.g. for $c = 1.73$, $d = 0.0172$, $f_0 = 0.0368$, $K = 682$, $u = 0.994$, $v = 0.0193$, $w = 6.08$, $\alpha = 4.15 \times 10^{-6}$). In the direct transmission model, higher v can increase host density but via a different mechanism. With environmental transmission, higher v increases conversion of infected hosts into parasite propagules, Z (leading to lower foraging rate). With direct transmission higher v reduces density of infected hosts (I) and reduces the spread of infection. Thus, with or without foraging depression, higher v can lead to higher host density

(Anderson 1979) by reducing disease (e.g., higher host density: $c = 1$, $d = 0.05$, $f_0 = 0.03$, $K = 50$, $u = 1$, $w = 1$, $\alpha = 0$ and $v = 0.4$ than for $v = 0.3$). So, through a foraging depression mechanism, a model of direct transmission (equation S6) produces similar hydra effects as that with environmental transmission (equation 1). However, virulence mortality (v) can increase host density by a different mechanism in the two models.

Section 2: Empirical methodological information

(a) Estimates of foraging depression (α) - Foraging rate assays – Fig. 1

We estimated coefficients of foraging depression (α) with short-term assays of foraging rate. In these assays, we reared cohorts of individuals of a genotype until they reached five days old. Then, we separated them into 15 mL tubes receiving 1.0 mg mass/L *Ankistrodesmus falcatus* (~70 μg chl *a*/L). Foraging depression for genotypes 1 and 2 was measured in one experiment (Strauss *et al.* 2019) while those of genotype 3 were measured in a separate but similar experiment (unpublished until now). For genotypes 1 and 2, each tube received a dose of 0 (N = 40 and 13, respectively), 75 (27 and 14), 200 (29 and 11), or 393 (38 and 14) parasite spores/mL. This high parasite propagule density likely corresponds to densities in large epidemics in nature (Tara Stewart Merrill personal communication). A separate experiment for genotype 3 had different assay durations and spore treatments (but all else equal). These foraging rate assays lasted 2, 5, or 8 hours. These time differences did not affect estimated foraging rates, so we combined them at 0 (N = 36) and 400 spores/mL (N = 36).

Despite these minor differences in design, both experiments then followed the same basic format. Control tubes interspersed through the experiment received the same treatment (i.e., algal density and spore dose) but without a zooplankton individual. All tubes were inverted

414 approximately every 30 minutes while kept in the dark for up to 8 hours. At the end of the
415 experiment, we removed animals, then measured remaining algae via *in vivo* fluorescence for
416 control and treatment tubes with a Turner Trilogy Laboratory Fluorimeter. For each individual S
417 (1 host /15 mL), we determined foraging rate [$f(Z)$] from the algae remaining in the treatment
418 tube (R_f) compared to the corresponding control tube (R_0) and the time lapsed, t_E [i.e. $f = \ln(R_0/R_f)/(S\,t_E)$]. For a small number of tubes, algal concentration was higher for the treatment
420 tube than the control tube, either due to death of the animal or a molting event (more likely).
421 These pairings of treatment and control tube were eliminated from the analysis.
422 For each genotype, we then fit a model of foraging depression to the foraging rate data.
423 Using the non-linear least-squares fitting function in R (R Core Team 2019), we fit foraging rate
424 as a function of spores, Z (following Strauss *et al.* 2019): $f(Z) = f_0 e^{-\alpha Z}$, where f_0 is the foraging
425 rate without spores (Z=0), and α is the coefficient of foraging depression (Fig. 1, used for model
426 equation 1). We found 95% confidence intervals for each genotype's α by bootstrapping (10^4
427 times). To bootstrap α for each genotype, we constructed sample datasets, retaining dataset size,
428 by randomly sampling foraging rate-spore density pairs within genotype and with replacement.
429 We then estimated confidence intervals from the distribution of α values fit to each bootstrapped
430 dataset (following Efron & Tibshirani 1993).
431

432 ***(b) Mesocosm experiment***

433 Each mesocosm was housed in a 75-liter acid washed polyethylene tank in a climate-
434 controlled room held at approximately 21°C. We filled tanks to 50 L with 80% tap water (treated
435 with Kordon Amquel Plus and Novaqua plus) and 20% filtered (Pall A/E: 1 μm) lake water.
436 Water loss from evaporation was replaced with further additions during the experiment. Low

nutrient tanks received 5 μg L^{-1} P (as K_2HPO_4) with corresponding nitrogen (as $NaNO_3$) while high nutrient tanks received 50 μg L^{-1} P; N:P ratio was 20:1 by mass. Nutrients were replenished twice weekly throughout the experiment to account for an estimated (exponential) 5% per day loss rate. All tanks were inoculated with 2 mg (by dry weight) of the green alga *Ankistrodesmus falcatus* 7 days before hosts were introduced (algae on day -6, hosts on day 1) and allowed to grow on a 24 hr light cycle to reach a high enough algal density to support hosts.

We added hosts to each tank on day 1 (10 hosts L^{-1}); hosts then grew 27 days before addition of 4660 fungal spores L^{-1} (day 28) to the disease treatment tanks. Isoclonal host lines obtained from Midwestern (MI, USA) lakes were cultured in the laboratory while spores (from Baker Lake, Barry Co, MI, USA) were cultured by passage through live hosts. Genotype 1 was 'Bristol 10', genotype 2 was 'A4-3', and genotype 3 was 'Standard'. Tanks received a 16 L: 8 D light cycle after host addition. Twice a week on days 14-86, we sampled 1 L of tank water, sieving animals through 80 μm mesh to destructively sample hosts. We visually counted and diagnosed hosts for infection using dissecting microscopes (40-50X).

(c) Determining experimental densities – Figs. 5, S7, S8

Several outliers in the experimental mesocosm populations were removed from the analyses. The majority were removed due to extinction of the host population, most often at low nutrients. The following were removed due to extinction:

- genotype 2: 2 at low *K*, *Z*-; 1 at low *K, Z*+
- genotypes 2&3: 1 at low *K, Z*-; 1 at low *K*, *Z*+
- genotype 3: 1 at low *K*, *Z*+

- genotype 1: 1 at high *K*, *Z*-

Future modeling work may account for stochastic extinction to gain insight from these populations. Another population (genotypes 2&3, low *K*, *Z*-) was removed due to contamination with the focal fungal parasite at an unknown date. One population of genotype 1 with high nutrients and parasites present was removed due to extremely low host density, possibly due to chemical contamination. This population's Cook's distance was > 4X the mean for host density (corresponding to 95th percentile); such a deviation is uncharacteristically low for this genotype, even at lower nutrient supply (J. Walsman, personal observation).

Population averages were taken over a 28-day time window (days 48 – 76) to best estimate quantities relevant to our theoretical models. On day 48, most populations in disease treatments (inoculated day 28) began to display sufficient visible infections. We ended on day 76 based on visual inspections of mesocosms and previous experiments. Around this time, mesocosms accumulate detritus and dynamics become less consistent across replicates. Then, over this 28-day window (several generations of hosts), we calculated averages as area under the curve divided by time. These averages provide closest comparison to model equilibria (equation 2).

(d) Nutrients and susceptibility increase prevalence in experimental populations – Fig S7

The model predicts that increased resource carrying capacity (*K*) and host susceptibility (*u*) increase prevalence. This pattern holds with foraging depression in the model (see results of numeric search in Appendix: Section 1b) and only grows stronger with a negative correlation between *u* and foraging depression. We tested the statistical effects of nutrients and susceptibility on prevalence with a beta regression. While a linear model finds the same qualitative result, a

beta regression is better suited for prevalence, which is bounded between zero and one (Ferrari & Cribari-Neto 2004; Mangiafico 2016). We implemented the beta regression using the betareg package (Cribari-Neto & Zeileis 2010) in Rstudio (R Core Team 2019) and the default "logit" link function. Diagnostic plots (following Ferrari & Cribari-Neto 2004) supported the use of the beta regression. The regression indicated that susceptibility (P = 0.0067) and nutrients (one-sided P-value = 0.0198) both increased prevalence.

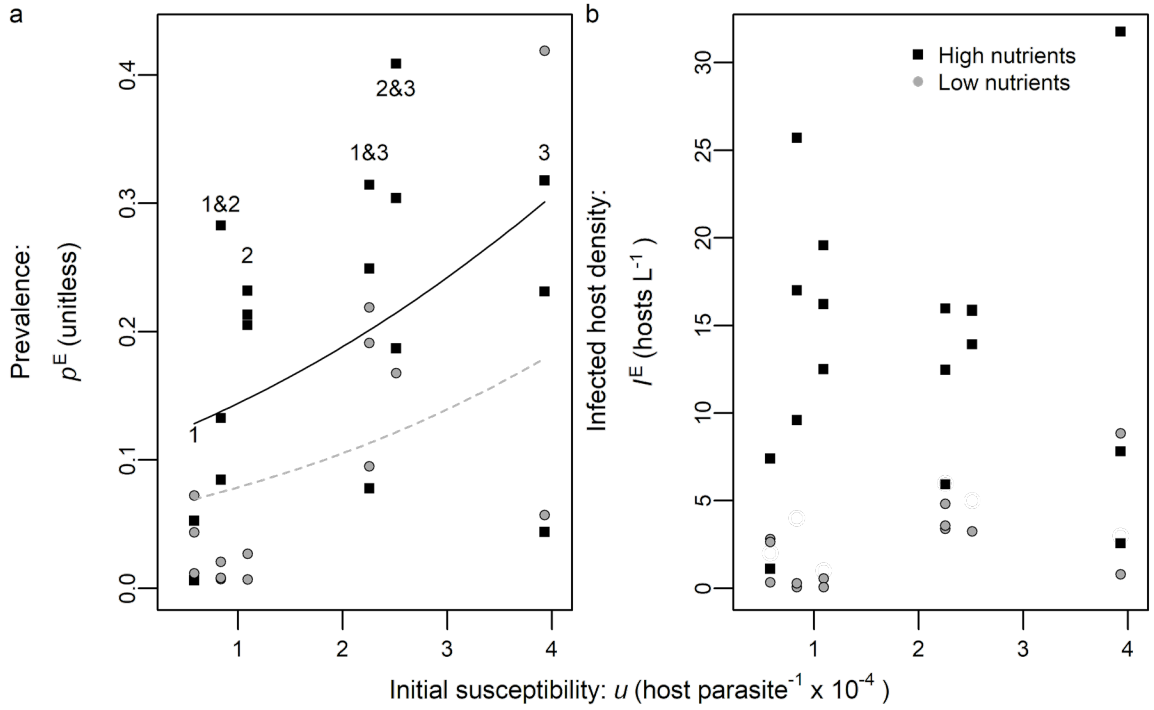

Figure S7. *Prevalence of infection and density of infected hosts in mesocosms.* Each point is a mesocosm population averaged over time. Gray circles: low nutrients; black squares: high nutrients. Vertical groupings are genotype treatments (with number labels on top). With increasing initial susceptibility (u) and nutrients (K), (a) prevalence (p^E) increases. (b) Infected host density (I^E) can reach high density compared to initial infection dose (~equivalent to two

496 infected hosts per 50 L, or 0.04 L^{-1}). This increase in infection density demonstrates that parasite
497 epidemics were self-sustaining in experimental populations.
498
499 Experimental mesocosms experienced self-sustaining, multi-generational epidemics of
500 varying sizes. In some populations, especially those with high susceptibility to infection (see beta
501 regression), nearly half of the population became infected (Fig. S7a). Epidemics were initialized
502 with 4,660 spores/L or 233,000 spores/population. This is roughly equivalent to the spores
503 released from two heavily infected hosts per population. Many disease populations attain a
504 density of infected hosts greater than 10/L (see Fig. S7b). With 50 L populations, this
505 corresponds to more than 500 infected hosts/population. Thus, initial infections (of animals
506 reared to produce spores used to inoculate mesocosms) resulted in secondary and (very likely)
507 tertiary infections, creating self-sustaining parasite epidemics. These self-sustaining parasite
508 epidemics distinguish our laboratory experiment from many others with one parasite generation
509 and/or donor-controlled parasite abundance. These less dynamic parasite populations are
510 tractable and useful for reducing experimental variation. But self-sustaining epidemics over
511 multiple host generations match assumptions of our dynamic model of feedbacks between
512 interacting populations of parasites, hosts, and resources. Perhaps more importantly, these
513 dynamic feedbacks more closely resemble those during epidemics in nature. Furthermore, such
514 feedbacks (especially for resources) are required to produce the hydra effect.
515 Infected host density can also help approximate parasite propagule densities. The model
516 predicts equilibrium parasite propagule density as $Z^* = \sigma(d+v)I^*/m$ (from equation 1d). Given
517 reasonable parameter values (see Table 1), 30 infected hosts/L (population average of upper right
518 point in Fig. S7b) corresponds roughly to 1.15×10^5 spores/L. The highest transient infected host

density observed in any treatment in the epidemic window was 82 infected hosts/L. Assuming the conversion is still roughly appropriate, this corresponds to 3.14 x 10^5 spores/L. Thus, the span of spore doses used in the foraging depression assay (see Fig. 1) likely corresponds to the range of parasite propagule densities host experienced in the mesocosms.

(e) Mapping model results onto predictions of main effects and interactions – Table S1

Whether or not foraging depression is present in the model, the model predicts the same main effects and interactions for disease, nutrients, and susceptibility. Higher susceptibility should always strengthen resource release and host suppression (Figs. 3c, d). Higher carrying capacity of the resource should always strengthen resource release (Fig. 3a) and may strengthen or weaken host suppression (only the weaken case is shown in Fig. 3b). Given trait measurements, disease should usually decrease host density and should always increase resource density (see Fig. 3). Meanwhile, higher carrying capacity should weaken host suppression (Fig. 3b).

We tested the effects of disease and its interactions with susceptibility and nutrients (resource carrying capacity) on experimental resource and host density. Each data point is the average for a given population in a unique mesocosm, ensuring independence of observations. We fit a linear model (equation S7) to $\log_{10}$ resource and host density in Rstudio (R Core Team 2019). Diagnostic plots supported the assumptions of linearity, homoscedasticity, and normally distributed error.

We found the effects of treatments on experimental resource (R^E) and host (H^E) densities using linear model fits to $\log_{10}$ mesocosm densities. The models take the following form:

$$\log_{10}(R^E) = r_0 + r_K K + r_u u + r_Z Z + r_{KZ} KZ + r_{uZ} uZ + \varepsilon_R \quad \text{(S7a)}$$

$$\log_{10}(H^E) = h_0 + h_K K + h_u u + h_Z Z + h_{KZ} KZ + h_{uZ} uZ + \varepsilon_H \quad \text{(S7b)}$$

We modeled $\log_{10}$ resource (R^E; equation S7a) or host (H^E; equation S7b) density in the experiment as a function, from left to right, of an intercept (r_0 and h_0), nutrients (represented by carrying capacity, K), susceptibility (u), and disease (Z) with K x Z (KZ) and u x Z (uZ) interactions and an error term (ε_R or ε_H following a Gaussian distribution). To aid interpretation of regression coefficients (i.e., the r and h parameters for resources and hosts, respectively), we centered the independent numerical variables (K and u) to have mean zero. Thus, we used values above or below the mean (zero) to predict the variable's effect on density. Then, for the categorical disease variable, we used a coding scheme that more naturally matched predictions of the differential equation model (equation 1). That model did not predict meaningful overall effects of u on density; hence, we did not code disease a more traditional way (which would fit main effects of K and u to the data overall, i.e. Z- = -1 and Z+ = 1). Instead, we coded the categorical disease treatment so that no disease (Z-) is 0 and disease (Z+) is 1. Therefore, no disease is the default in this linear model; the main effects of K and u are provided without disease. This choice, then, allowed comparison to clear predictions.

Mapping theory predictions onto fitted coefficients is straight-forward because the derivative of equilibrium density (on an arithmetic scale) has the same sign as the derivative of $\log_{10}$ density. For example, higher carrying capacity (K, related to increased nutrients for algae) increases equilibrium host density in the absence of parasites ($\mathrm{d}/\mathrm{d}K\ H^*_{Z-} > 0$; derived from equation 2c). Thus, K must also increase $\log_{10}$ host density [$\mathrm{d}/\mathrm{d}K\ H^E_{Z-} > 0$ implies $\mathrm{d}/\mathrm{d}K$ $\log_{10}(H^E_{Z-}) = h_K > 0$; equation S7b]. The same logic predicts the signs of other regression coefficients: $r_K = 0$, $r_u = 0$, $h_u = 0$ (see theory predictions and experimental outcomes compared in Table S1).

Similarly, the model predicts main effects of the categorical disease treatment and its interactions. The model predicts disease will increase resources ($R^*_{Z+} > R^*_{Z-}$; $r_Z > 0$) and usually decrease host density ($H^*_{Z+} < H^*_{Z-}$; $h_Z < 0$). Interaction effects are predicted by how a variable (carrying capacity K or susceptibility u) influences density ratio. For example, host density ratio decreases with susceptibility in the model [d/du (H^*_{Z+}/H^*_{Z-}) < 0 because H^*_{Z+} decreases with u, Fig. 3d]. Thus, $\log_{10}(H^*_{Z+}/H^*_{Z-})$ also decreases with u. A negative effect of u on $\log_{10}$ host ratio equates to $h_{uZ} < 0$. Thus, there should be a negative interaction between susceptibility and disease for host density because the model predicts parasite-driven host suppression is stronger when hosts are more susceptible.

The model predicts most features of resource release in the experiment. The addition of disease significantly increased resources (Fig. S8a, b). Susceptibility to infection (u) had no impact on algal density without disease (flat gray line Fig. S8b). But, as predicted, resource release was magnified by higher susceptibility (positive u x Z interaction; black slope higher than gray in Fig. S8b and increasing resource ratio in Fig. 5a). All of these results were consistent with predictions (Table S1). However, a few small inconsistencies between model and experiment also arose. The effect of nutrient supply on resources differed somewhat from that predicted by the model equilibrium, likely due to transient dynamics. In the model at equilibrium and without disease, hosts graze resources down to their minimum resource requirement, which does not depend on resource carrying capacity (equation 2a). Before reaching equilibrium, transient resources can increase with carrying capacity until hosts depress resources to the hosts' minimal requirement. This pattern likely explains why, in the mesocosms, algal resources in the absence of disease (R^E_{Z-}) increased somewhat with nutrient supply (significant positive effect of K; see Fig. S8a, Table S1). That increase of resources with nutrient supply likely also weakened

588 the *K* x *Z* interaction for resources. Thus, the treatment effects on algal density were largely (but
589 not entirely) consistent with the model.

590 The model largely predicts drivers of host suppression as well. Higher nutrient supply (*K*)
591 should and did increase host density (H^{E}_{Z-}) without disease (Fig. S8c, Table S1). Counter to the
592 model, higher susceptibility (*u*) did increase host density without disease (positive gray slope
593 Fig. S8d). This relationship might have arisen due to differences in non-focal traits of these
594 genotypes (Strauss et al. 2015). Nonetheless, parasites suppressed host density (Fig. S8c, d).
595 Host suppression weakened non-significantly with higher nutrient supply (i.e., non-significant,
596 positive *K* x *Z* interaction for host density). Higher susceptibility, as predicted, did amplify host
597 suppression (negative *u* x *Z* interaction, as predicted; black line [*Z*+] had lower slope than gray
598 line [*Z*-] in Fig. S8d and decreasing host ratio in Fig. 5b). So, susceptibility strengthened host
599 suppression while nutrient supply did not significantly affect it (Fig. 5b).
600

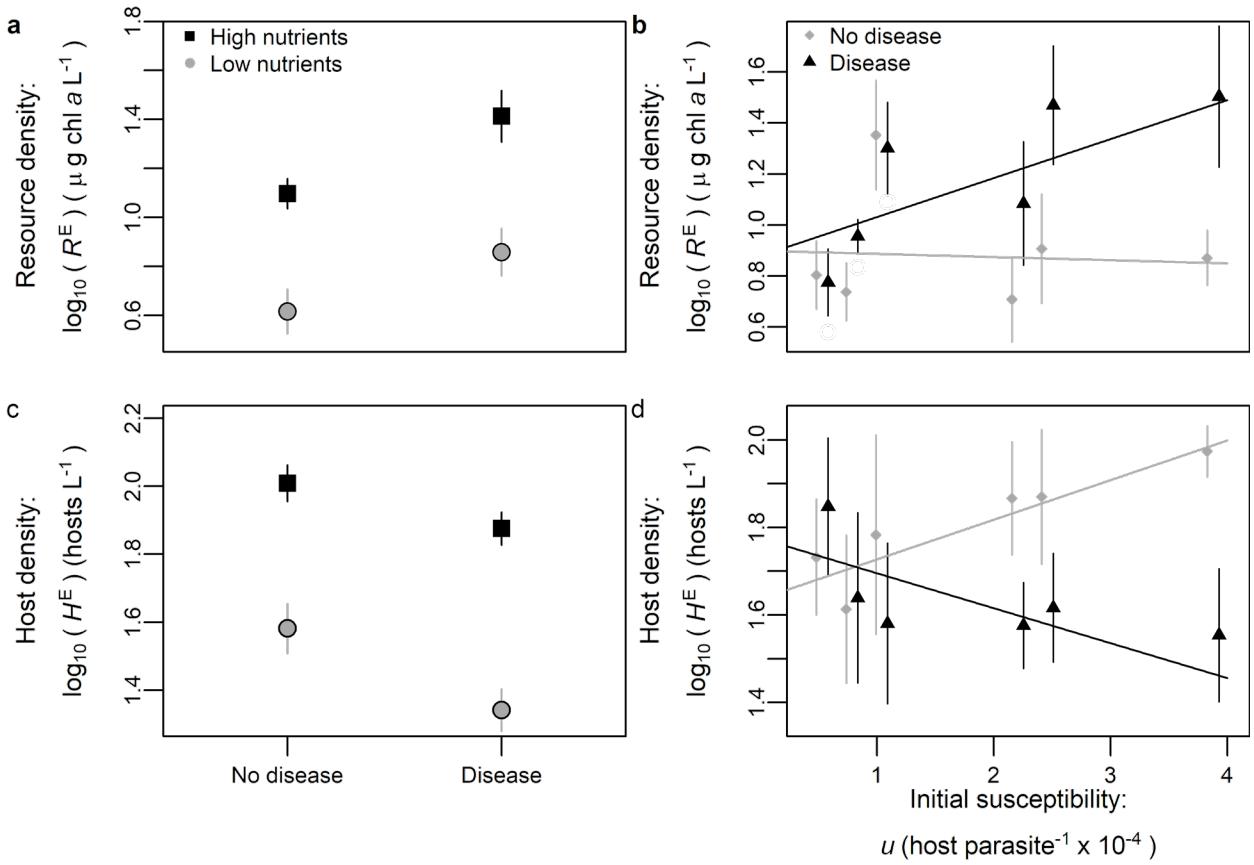

601

602 **Figure S8.** *Parasites drive cascades modulated by susceptibility more than carrying capacity.*
603 Each point represents an average over time and populations within a group of treatments of $\log_{10}$
604 density. First column is grouped by nutrient supply and disease treatment. Nutrient supply
605 treatments: high (black squares) and low (gray circles; see text). Susceptibility (u) was
606 manipulated using one of three single-genotypes (1, 2, or 3) or (initially) a 50:50 mixture of two
607 (e.g. 1&2), creating a range of u. *Algal resources*: (a) Nutrient supply (K) and disease (Z+)
608 increase experimental resource density (R^E; compare Fig. S1c) with no interaction (see Table
609 S1). Second column is grouped by susceptibility and disease treatment. (b) Susceptibility does
610 not affect resource density without disease (diamonds along flat gray line) but increases
611 resources with disease (triangles increasing with black line; as in Fig. S1c; u x Z interaction).
612 *Plankton hosts:* (c) Nutrient supply increases and disease decreases host density (H^E; as in Fig.

S1e) with no interaction. (d) Susceptibility increases host density without disease (diamonds along gray line) but decreases it in the presence of disease (triangles along black line; compare Fig. S1e; u x Z interaction). Note that panels b and d are collapsed by nutrients so the hydra effect at high nutrients is less visible. Bars are standard errors.

Table S1. *The model (eqs. 1, 2) largely predicts GLM treatment effects in a mesocosm experiment*. Theoretically predicted or experimentally determined effects of nutrient supply (K), host susceptibility (u), or disease (Z+) treatments (Trmt) on resource (R) or host (H) density. Here, disease-free (Z-) treatments are the default. Hence, main effects of K and u denote their effects without disease. A '+/-' means that theory predicts a potential positive or negative effect while NS denotes non-significant results (e.g. "NS+" is a non-significant positive trend). Theoretical predictions are drawn from equilibrium densities (equation 2) mapped onto GLM coefficients (see Appendix: Section 2e). Many of the predictions are general but some depend on biologically relevant parameter values. Experimental ('E') values are parameter estimates (r_i, h_i) from a linear model (equation 2) predicting $\log_{10}$ mean experimental density (R^E and H^E) averaged over time and treatment. P-values are provided.

Trmt	**Resources (*R*)**			**Hosts (*H*)**		
	Theory R^*	**Exp. R^E**	**P-value**	**Theory H^***	**Exp. H^E**	**P-value**
K	d/dK R^*_{Z-}: **0**	0.011	2 x 10^{-4}	d/dK H^*_{Z-}: +	0.0095	6.3 x 10^{-7}
u	d/du R^*_{Z-}: **0**	-0.012	0.806	d/du H^*_{Z-}: **0**	0.091	0.006
Z	$R^*_{Z+} > R^*_{Z-}$	0.290	0.001	$H^*_{Z+} < H^*_{Z-}$	-0.182	0.001
K* x *Z	d/dK R^*_{Z+}/R^*_{Z-}: +	0.0008	0.841	d/dK H^*_{Z+}/H^*_{Z-}: +/-	0.0029	0.241
u* x *Z	d/du R^*_{Z+}/R^*_{Z-}: +	0.165	0.028	d/du H^*_{Z+}/H^*_{Z-}: -	-0.171	0.0005

630 ***(f) Statistical significance of experimental hydra effects – Fig. 5***

631 Host density appeared to be higher with disease than without disease (a hydra effect) for
632 treatments with high nutrient supply and with host genotype 1 or genotypes 1 and 2 combined.
633 Necessary removal of outlier populations (see Appendix: section 2c) and the occurrence of a
634 hydra effect for only certain genotypes provided a small number of replicate populations (2 with
635 parasites and 2 without for genotype 1; 3 with parasites and 3 without for genotypes 1&2). Nine
636 repeated measurements of each population over time provide additional statistical power. But
637 these repeated measurements are autocorrelated. To account for this autocorrelation, we used a
638 nested ANOVA, with time nested within individual mesocosm and individual mesocosm nested
639 within disease treatment. We performed the nested ANOVAs in R (R Core Team 2019) with host
640 density and log host density. Host density (whether or not it was log transformed) was
641 significantly higher with disease for both genotype treatments. However, the homoscedasticity
642 assumption of nested ANOVAs, as diagnosed with a residuals vs fitted plot, was satisfied better
643 by log-transformed host density. Normal Q-Q plots also revealed residuals of log-transformed
644 host density to be approximately normal for both genotype treatments. Thus, we report results for
645 log host density. As reported in the text, host density was significantly higher with disease than
646 without disease for genotype 1 alone ($P = 0.007$) as well as the mixed genotype 1 and 2 treatment
647 ($P = 0.020$).

648

649 **References**

650 Anderson, R.M. (1979) Parasite pathogenicity and the depression of host population equilibria.
651 *Nature,* **279,** 150-152.

Cribari-Neto, F. & Zeileis, A. (2010) betareg: Beta Regression in R. *Journal of Statistical Software,* **32,** 1-24. 10.18637/jss.v034.i02

Ebert, D., Lipsitch, M. & Mangin, K.L. (2000) The effect of parasites on host population density and extinction: Experimental epidemiology with Daphnia and six microparasites. *American Naturalist,* **156,** 459-477. 10.1086/303404

Efron, B. & Tibshirani, R.J. (1993) *An Introduction to the Bootstrap*. Chapman & Hall, New York.

Ferrari, S. & Cribari-Neto, F. (2004) Beta regression for modelling rates and proportions. *Journal of applied statistics,* **31,** 799-815.

Mangiafico, S.S. (2016) *Summary and Analysis of Extension Program Evaluation in R, version 1.18.1.*

McKay, M.D., Beckman, R.J. & Conover, W.J. (2000) A comparison of three methods for selecting values of input variables in the analysis of output from a computer code. *Technometrics,* **42,** 55-61.

R Core Team (2019) R: A language and environment for statistical computing. R Foundation for Statistical Computing, Vienna, Austria.

Shurin, J.B., Borer, E.T., Seabloom, E.W., Anderson, K., Blanchette, C.A., Broitman, B., Cooper, S.D. & Halpern, B.S. (2002) A cross-ecosystem comparison of the strength of trophic cascades. *Ecology Letters,* **5,** 785-791. 10.1046/j.1461-0248.2002.00381.x

Shurin, J.B. & Seabloom, E.W. (2005) The strength of trophic cascades across ecosystems: predictions from allometry and energetics. *Journal of Animal Ecology,* **74,** 1029-1038. 10.1111/j.1365-2656.2005.00999.x

674 Strauss, A.T., Hite, J.L., Civitello, D.J., Shocket, M.S., Cáceres, C.E. & Hall, S.R. (2019)
675 Genotypic variation in parasite avoidance behaviour and other mechanistic, nonlinear
676 components of transmission. *Proceedings of the Royal Society B,* **286,** 20192164.

677